Bifacial crystalline silicon homojunction cells contacted with highly resistive TCO layers

Elise Bruhat, Thibaut Desrues, Bernadette Grange, Danièle Blanc-Pélissier, Sébastien Dubois

Bifacial Crystalline Silicon Homojunction Cells Contacted with Highly Resistive TCO Layers

Elise Bruhat[1, a)], Thibaut Desrues[1], Bernadette Grange[1], Danièle Blanc-Pélissier[2] and Sébastien Dubois[1]

[1]*Univ. Grenoble Alpes, INES, F-73375 Le Bourget du Lac, France CEA, LITEN, Department of Solar Technologies, F-73375 Le Bourget du Lac, France*
[2]*Université de Lyon, Institut des Nanotechnologies de Lyon INL - UMR5270, CNRS, Ecole Centrale de Lyon, INSA Lyon, Villeurbanne, France*

[a)]Corresponding author: elise.bruhat@cea.fr

Abstract. This study explores the needed properties of Transparent Conductive Oxides (TCOs) for bifacial homojunction solar cells with potentially passivated contacts. TCO layers with different electrical and optical properties have been tested on both sides of n-type homojunction cells. The high lateral conductivity provided by the diffused emitter and back surface field (BSF) greatly reduces the constraints on TCO electrical properties in such structures. An understanding of the required properties of TCO for advanced homojunction applications is given. Hence different O2-rich Indium Tin oxide (ITO) layers are analyzed optically and electrically before being implemented in homojunction solar cells to evaluate their influence on the device performances. All in all moderately conductive TCOs are shown to be suitable for such applications, allowing better optical properties without inducing resistive losses in the devices.

INTRODUCTION

Most crystalline silicon (c-Si) homojunction solar cells present highly doped regions at the c-Si surfaces with a direct contact between the c-Si and the metal grid thus promoting electron-hole recombinations (see Fig. 1a). In order to obtain higher open circuit voltage (V_{OC}) and lower saturation current densities (J_0) "lightly doped homojunctions" [1,2] approaches are being considered. However to overcome recombination issues due to the direct contact between the doped c-Si and the metal grid, and to counterbalance the higher sheet resistance (R_{Sheet}) of lowly doped emitters, TCO layers may be used (see Fig. 1b)[3,4]. In addition to being conductive and antireflective, TCO layers can act as passivating layers. Such passivating properties can be obtained thanks to either hydrogenation of the TCO or in combination with a passivating ultra-thin underlayer[5,6] (see Fig. 1c). The aim of this preliminary study is to get new insights into the resistive losses due to the interaction of TCO with homojunction dopings, therefore no passivating layers are introduced in this study.

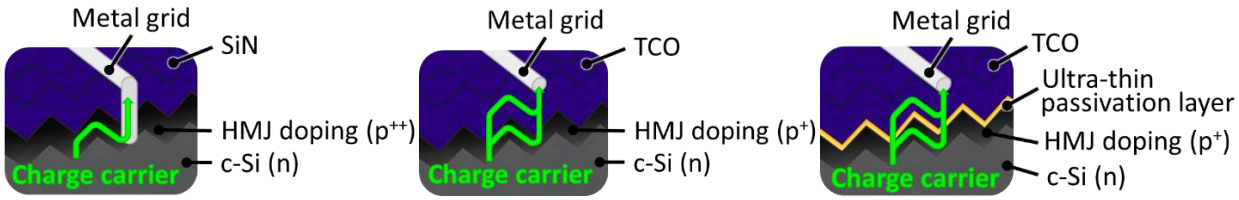

FIGURE 1. Standard contact for homojunction silicon solar cells (a), a TCO-related contact (b) and a TCO/ultra-thin passivation layer (c).

High resistivity collectors (a-Si:H, thin poly-Si) require the use of TCO layers featuring high conductivity values to improve both the lateral charge transport and the charge collection by metal electrodes. However TCO layers with high conductivity values usually feature poor optical properties (i.e, light absorption).

For homojunction applications, high lateral conductivity is already achieved thanks to the c-Si over-doping at the surfaces[1]. Thus it could be asked if TCOs with high conductivity are still needed or if another optimum between optical and electrical properties of the TCO layer could be considered. In order to bring new insights into the influence of the charge collector (i.e, highly doped c-Si here) lateral conductivity on the TCO features for homojunction solar cells, different Indium Tin Oxides (ITO) were tested with dopant-diffused c-Si wafers. It should be noted that no surface passivation layer (e.g, tunnel layer) between the TCO and the c-Si wafer is used in this study, thus reducing the short circuit current density (J_{SC}) and V_{OC} performances.

MATERIALS & METHOD

Industrial 156×156 mm² n-type pseudo-square Cz-Si wafers (ρ_{Sibulk} = 4.1 Ω.cm) were prepared using a wet chemical texturing process. After thermal diffusion doping of the samples ($R_{Sheet\_emitter/c\text{-}Si(n)}$ = 70 Ω/sq and $R_{Sheet\_BSF/c\text{-}Si(n)}$ = 57 Ω/sq) and a cleaning step, Magnetron Sputtering (MS) ITO layers (80 nm) were deposited at 200°C on both sides of the textured Si wafers. One side was coated with the same standard ITO (Oxygen pressure pO_2 = 4.5 sccm) while the electrical properties of the ITO deposited on the other side of the wafer were tuned thanks to different pO_2/pAr ratios (fixed pAr at 350 sccm). The coated c-Si wafers were then metallized using Ag screen printing (4 bus bars, 1.8 mm pitch, line resistivity of 7 μΩ.cm) and annealed 20 minutes at 200°C under air. Those experiments lead to two different cell structures (see Fig. 2), one with variable ITO properties on the front surface, and the second with variable ITO properties on the rear surface. In order to investigate their optical and electrical properties, ITO layers were also deposited on glass samples and annealed under the same conditions as the c-Si cells.

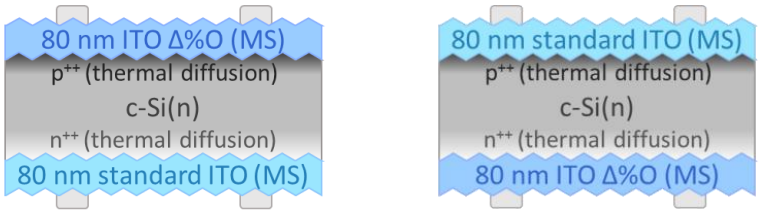

FIGURE 2. Structures of the cells

The R_{Sheet} values of the TCO layers were measured using a 4-point probe on both glass and c-Si substrates. On glass substrates, Hall effect measurements were used to determine the majority carrier density and mobility while optical spectroscopy was done to measure their absorption properties. To compare cells performances, illuminated I-V measurements were performed to extract the electrical photovoltaic parameters of the cells (V_{OC}, J_{SC}, Fill factor (FF). The conversion efficiency (η) was measured under 1-sun illumination (front emitter configuration). Finally, to check the quality of the contact between the TCO layer and the metal grid, Berger measurements were performed [7] on Ag/ITO/thick thermal-SiO_2/c-Si samples. In order to provide accurate results, all characterizations were made on at least two samples, and standard deviation was calculated to show value dispersion on graphs.

RESULTS

Properties of the ITO (MS) Layers with Different O_2 Ratios

As expected, the electrical analyses of the different ITO layers on glass show that increasing the amount of O_2 from 0.9 to 3.3% in the MS process increases the ITO layer R_{Sheet} from 100 to 400 Ω/sq. Annealing the layers slightly decreases their resistivity (by 15% roughly) but all trends are conserved (see Fig. 3a). Indeed, increasing pO_2 strongly decreases the carrier density down to $7x10^{19}$ cm^{-3} while slightly increases their mobility up to 32 cm^2/Vs (Fig. 3b). When applying those different layers on the dopant-diffused c-Si wafers, similar trends are observed: R_{Sheet} of the ITO/emitter/c-Si(n) stack being lower than the initial R_{Sheet} of the emitter (70 Ω/sq) or BSF (57 Ω/sq). Thus all the tested ITO layers are conductive enough to improve the overall carrier transport within the cells. The effective

absorptions in the visible light and the infrared region (Fig. 4) also show an increase of the transparency of ITO with the percentage of O_2 during the MS process as shown in previous studies [8,9].

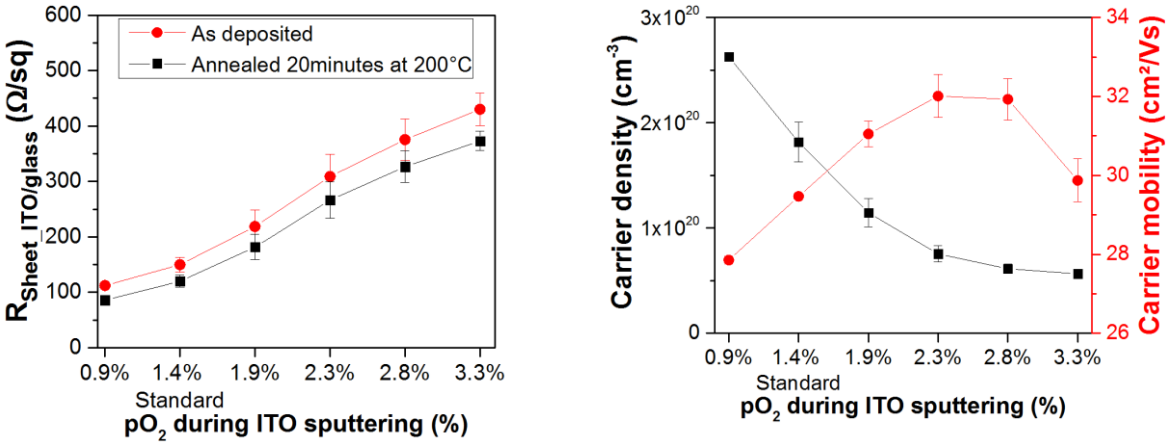

(a) (b)

FIGURE 3. Variation of ITO sheet resistance values on glass samples for different pO_2 before and after the annealing step (a) and associated carrier mobility and density for ITO annealed 20 minutes at 200°C (b).

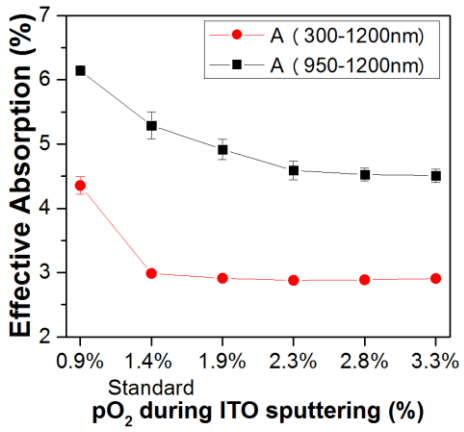

FIGURE 4. Variation of the effective absorption of ITO in the visible light and infrared region for different pO_2 concentrations.

Series resistance issues due to ITO layers

Study of the ITO/c-Si interface

As the sheet resistance of the ITO layer increases with pO_2 injected during the sputtering process, one can question first the ability of the charges to flow from the heavily doped c-Si to the ITO. To understand such interactions, 4-point probes measurements were performed on the precursors after ITO deposition (Fig. 5a).

As the TCO has a higher sheet resistance than the doped region, if the carrier flow was confined within the TCO, the sheet resistance measured in this experiment would be that of the ITO[2]. Performed measurements show that even though an increase in sheet resistance of ITO/c-Si exists with increasing pO_2, the sheet resistance of the stack stays below the initial sheet resistance of the doped layer ($R_{Sheet\_emitter/c\text{-}Si(n)}$=70 Ω/sq). Thus the contact resistance between the ITO and the highly doped c-Si layer is sufficient for the current to flow across both the TCO and the c-Si substrate. Same results are obtained for the BSF/ITO contact (not shown here).

Series resistance (R_S) losses for such ITO/emitter stacks can be calculated (1) and are comparable with an increase of R_S between ITO(pO_2=0.9%) and ITO(pO_2=3.3%) of ΔR_S=0.04 Ω.cm² which is equivalent to a loss of 0.2% absolute in FF[10]. Moreover, simulations made for ITOs deposited on highly resistive junctions show that higher sheet

resistances of the stack ITO/emitter would lead to higher losses in series resistances up to 0.2 Ω.cm², leading to an overall loss of 1% in FF from $R_{Sheet\_emitter/c\text{-}Si(n)}$=70 Ω/sq to $R_{Sheet\_emitter/c\text{-}Si(n)}$=200 Ω/sq for an ITO at pO_2=3.3%.

$$R_{series\_ITO/emitter} = \frac{1}{3} R_{Sheet\_ITO/emitter} \left(\frac{\text{metal grid pitch}}{2}\right)^2 \quad (1)$$

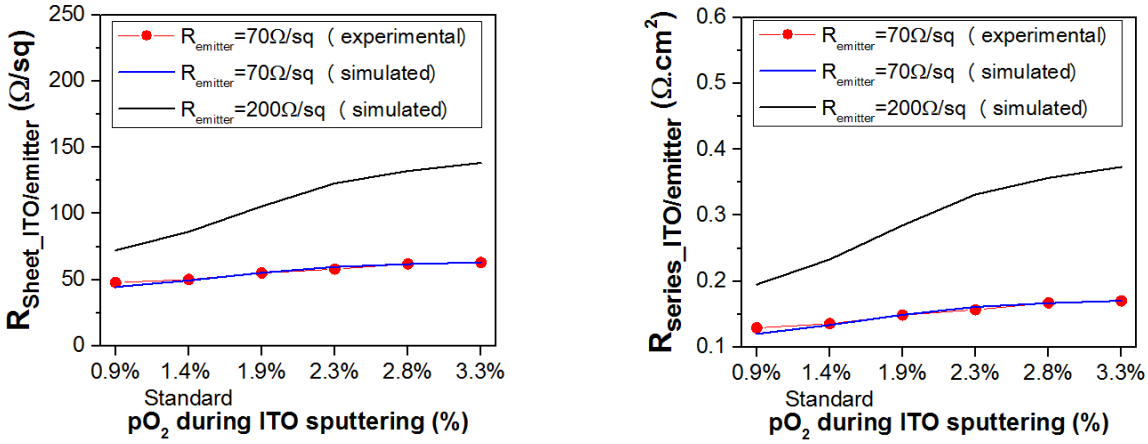

(a) (b)

FIGURE 5. Variation of the sheet resistance of the ITO/doped c-Si with pO_2 for different $R_{Sheet\_emitter}$ (a) and its impact on series resistance (b).

Contacting the Different ITO Layers

Contact resistivity ($\rho_{contact}$) between the metal grid and the ITO for all pO_2 concentrations are extracted form Berger measurements (Fig. 6). After the metal grid deposition, high $\rho_{contact}$ are measured. However, a 20 minutes annealing step at 200°C allows all contact resistivity to drop thus helping current collection for all samples. A longer annealing or at higher temperature could eliminate all resistive losses due to the metal/ITO contact for the cells if $\rho_{contact}$<3mΩ.cm² is achieved.

Again, series resistance losses linked to the increasing metal/ITO contact resistivity on highly doped junctions ($R_{Sheet\_emitter}$=70 Ω/sq) are small, ΔR_S=0.03 Ω.cm² which is equivalent to a loss of 0.15% in FF. Moreover, the variation of $R_{Sheet\_emitter}$ has also a low impact on the overall resistance losses as the difference between a lightly doped emitter and a resistive emitter is only of ΔR_S=0.04 Ω.cm² (0.2% loss in FF) for an ITO at pO_2=3.3%.

$$R_{series\_front\ contact} = \frac{\text{metal grid pitch}}{2} \left(\rho_{contact\ metal/ITO} \cdot R_{Sheet\_ITO/emitter}\right)^{1/2} \quad (2)$$

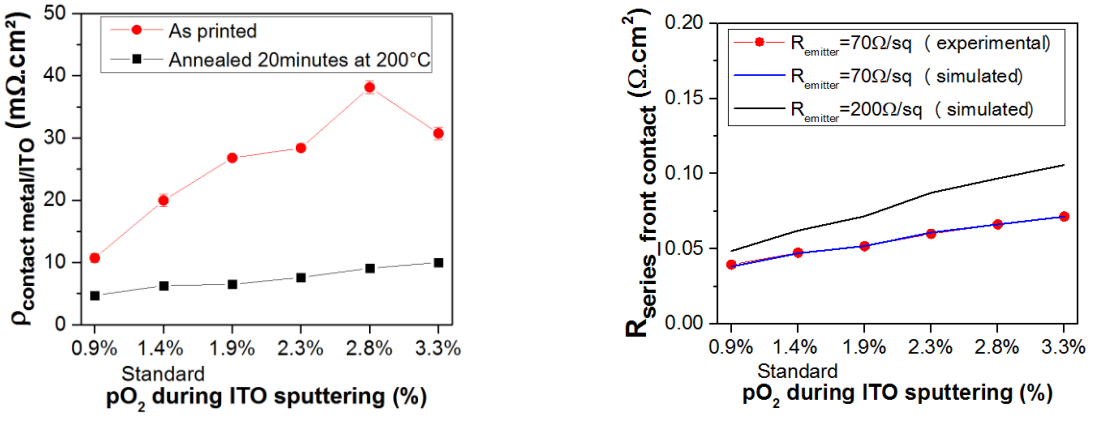

(a) (b)

FIGURE 6. Variation of the contact resistivity between the metal grid and the 80 nm thick ITO layers for different pO_2 concentrations (a) and its impact on series resistance for different $R_{Sheet\_emitter}$ (b).

Solar Cells Results

As expected low V_{OC} and J_{SC} values were obtained (Fig. 5 & 6), due to the lack of passivation layer in this study. However changes in the cell performances are still noticeable.

ITO Oxygen Variation on the Emitter Side

Enhancement of the J_{SC} and V_{OC} with the increase of pO_2 concentration during MS ITO deposition on the front side of the cell is noticeable (Fig. 7). The increase in V_{OC} might be related to a slight growth or morphological change of the native oxide with pO_2 or a change in work function (W_f) with the increased amount of ITO. The increase in J_{SC} is probably due to the lower absorption of ITO at high O_2 concentrations.

The fill factor is mostly influenced by the resistive losses. Therefore the increase of the ITO resistivity (higher O_2 concentrations) should lead to a decrease of the FF. Surprisingly, an increase is noticeable between pO_2 = 0.9% and pO_2 = 1.4% leading to think that the conductivity from the dopant-diffused regions to the overall conduction seems sufficient to reduce the constraints on the front TCO conductivity. However, fill factor performances are dropping for pO_2 > 1.4% probably due to the $\rho_{contact}$ at the metal/ITO interface. Still, for those oxygen-rich ITO the FF is slightly improving with pO_2 concentration. As this is contradictory with the variation in $\rho_{contact}$ it could be linked to a change in W_f of the ITO layer.

Thanks to good short circuit current performances, best cell are obtained with pO_2 = 3.3%. It is possible that a longer or higher temperature annealing might increase the properties of cells with higher O_2 concentrations as the contact between the metal grid and those ITOs is not optimal with a 20 minutes annealing steps (Fig. 6).

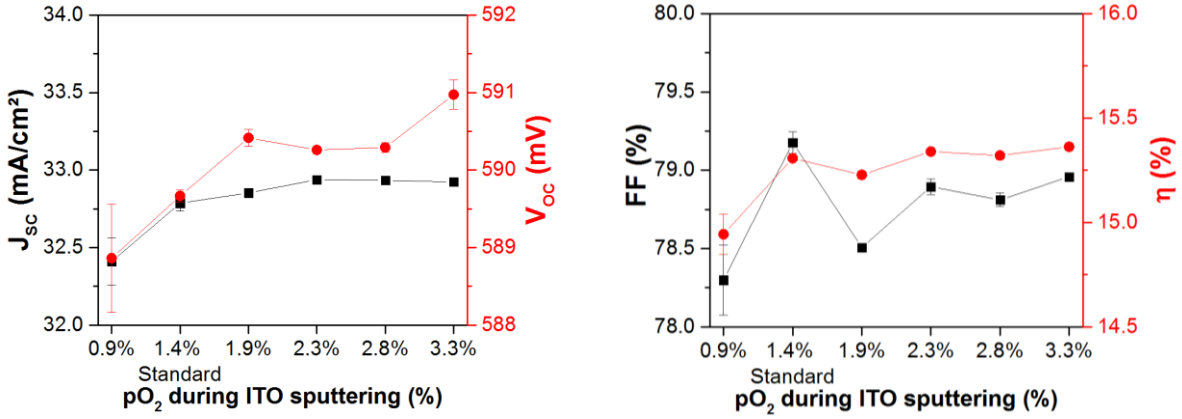

FIGURE 7. Variation of V_{OC}, J_{SC} (a), FF and η (b) with pO_2 for cells with different ITO composition on the front side of the annealed bifacial silicon solar cell.

ITO Oxygen Variation on the Rear Side

Analyses of the I-V measurements under illumination (Fig. 8) for cells with a varying ITO on the rear side show an enhancement of J_{SC} with the increase of pO_2 concentration during MS ITO deposition could be linked to the reduced absorption in the infrared region of the ITO (Fig. 4) coupled with a reflective chuck at the back of the cell during the I-V measurements. However, the sudden increase for $_{pO2}$=3.3% is not yet understood and further optical studies are ongoing. The V_{OC} variation with the pO_2 is opposite to when the changing ITO is on the front side, which may indicate a change in W_f with pO_2 concentrations.

Similar FF values are obtained for pO_2 concentrations below 2.8%. Thus the charge transport in the diffused c-Si regions, allows the use of TCO with lower conductivity values. Again, a longer annealing could increase the properties of cells with higher O_2 concentrations. In this case, best cell performances are obtained with pO_2 = 3.3% which is mainly due to the increase in J_{SC} attributed to the reflexion of the infrared light by the chuck. The ITO giving the lowest resistive losses is still pO_2 = 3.3% for a 20 minutes annealing at 200°C.

CONCLUSIONS AND PERSPECTIVES

- The TCO layer conductivity has a low influence on the global series resistance of homojunction devices, as shown by FF values up to 79% obtained using a 400 Ω/sq ITO layer
- If for high resistivity collectors the sheet resistance of the ITO layer needs to be below 150 Ω/sq, for homojunction devices the use of ITO layers with lower conductivity and absorbance can be used and even increase cells performances. The best cell performances being obtained for pO_2 = 3.3% during ITO deposition.
- The poor surface passivation properties of the ITO layers used in this study clearly limit cell performances (V_{OC} and J_{SC}), indicating a need to develop different TCO materials and/or stacks with "tunnel" oxides inserted between the c-Si and the TCO layer.

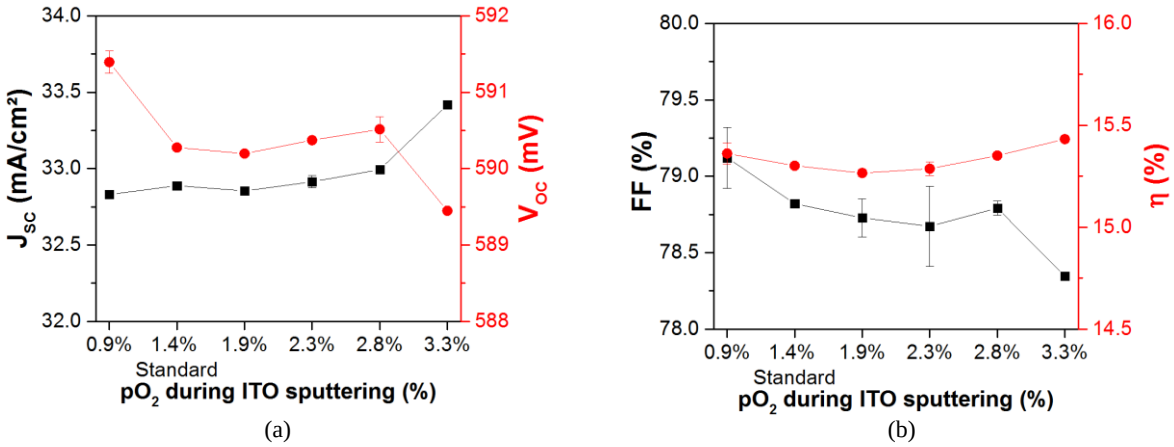

FIGURE 8. Variation of V_{OC}, J_{SC} (a), FF and η (b) with pO_2 for cells with different ITO composition on the rear side of the annealed bifacial silicon solar cell.

AKNOWLEDGMENTS

The team gratefully acknowledges Auvergne-Rhône-Alpes Region for financially supporting the project through the ARC4 program. This project has received funding from the French National Research Agency (Programs "Investment for the Future" ANR-10-ITE-0003 and "Oxygen" ANR-17-CE05-0035), and has also received funding from the European Union's Horizon 2020 research and innovation program under grant agreement No 727529.

REFERENCES

[1] R. Müller, J. Benick, N. Bateman, J. Schön, C. Reichel, A. Richter, M. Hermle, and S.W. Glunz, Sol. Energy Mater. Sol. Cells **120**, **Part A**, 431 (2014).
[2] G.G. Untila, T.N. Kost, A.B. Chebotareva, and E.D. Kireeva, Sol. Energy Mater. Sol. Cells **137**, 26 (2015).
[3] M. Kim, J. Kim, Y.-J. Lee, M. Ju, C. Park, N. Balaji, S. Lee, J. Kim, and J. Yi, Mater. Lett. **116**, 258 (2014).
[4] B. Min, J. Krügener, M. Müller, K. Bothe, and R. Brendel, Energy Procedia **124**, 126 (2017).
[5] J. Panigrahi, Vandana, R. Singh, and P.K. Singh, in *2016 IEEE 43rd Photovolt. Spec. Conf. PVSC* (2016), pp. 2964–2966.
[6] A. ur Rehman, M.Z. Iqbal, M.F. Bhopal, M.F. Khan, F. Hussain, J. Iqbal, M. Khan, and S.H. Lee, Sol. Energy **166**, 90 (2018).
[7] H.H. Berger, J. Electrochem. Soc. **119**, 507 (1972).
[8] M. Bender, W. Seelig, C. Daube, H. Frankenberger, B. Ocker, and J. Stollenwerk, Thin Solid Films **326**, 72 (1998).
[9] H. Askari, H. Fallah, M. Askari, and M.C. Mohmmadieyh, ArXiv Prepr. ArXiv14095293 (2014).
[10] D. Pysch, A. Mette, and S.W. Glunz, Sol. Energy Mater. Sol. Cells **91**, 1698 (2007).